Initiation of Localized Corrosion of Ferritic Stainless Steels by Using the Liquid-Phase Ion Gun Technique

Jun-Seob Lee,[a] Takashi Kawano,[b] Tomohiro Ishii,[c] Yuichi Kitagawa,[a] Takayuki Nakanishi,[a] Yasuchika Hasegawa,[a] and Koji Fushimi[a,*,z]

[a]*Faculty of Engineering, Hokkaido University, Kita-ku, Sapporo 060-8628, Japan*
[b]*Steel Research Laboratory, JFE Steel Corporation, Kawasaki-ku, Kawasaki 210-0855, Japan*
[c]*Steel Research Laboratory, JFE Steel Corporation, Chuo-ku, Chiba 260-0835, Japan*

The initiation of localized corrosion of types 430 and 443J1 ferritic stainless steels was evaluated in 0.15 mol dm^{-3} Na_2SO_4 solution. A liquid-phase ion gun (LPIG), a silver microelectrode covered with a silver chloride layer, was cathodically polarized to generate Cl^- in the vicinity of the stainless steel polarized at 0.4 V_{SSE}. Contact of the stainless steel surface with the Cl^--concentrated environment by the LPIG operation induced a rapid increase in anodic current flow through the stainless steel electrode after the induction period t_d and consumption of the cathodic electric charge Q_d by the LPIG microelectrode. Numerical modeling using the LPIG microelectrode current for t_d gave a critical Cl^- concentration $[Cl^-]_d$ needed for the initiation of localized corrosion. These parameters obtained by LPIG tests showed that type 443J1 stainless steel was superior to type 430 stainless steel in localized corrosion resistance. AES depth profiling of the stainless steel surfaces after the LPIG operation revealed enrichment of Cl in the outermost oxide film as well as decreased film thickness. The mechanism of degradation of the stainless steel surface due to contact with the Cl^--concentrated solution is discussed. The adsorption of Cl^- on the oxide surface is thought to be a trigger of the oxide degradation.

Manuscript submitted October 11, 2016; revised manuscript received November 28, 2016. Published December 8, 2016.

Stainless steel, an Fe-based material with a minimum of 11 wt% Cr content, has corrosion resistance, which is attributed to the formation of Cr- and/or Fe-oxide films, so-called passive films, on the surface. The resistance is related to the chemical composition of the film, which is strongly dependent on the chemical composition of the substrate. The pitting resistance equivalent (PRE) number (= wt% Cr + 3.3 (wt% Mo + 0.5 wt% W) + 16 wt% N) has been used to determine the localized corrosion resistance of stainless steel.[1] The larger the PRE number of stainless steel is, the greater is the resistance of the stainless steel to localized corrosion. The PRE number is related to the contribution of elements to the resistance of a passive film on stainless steel. Alloying with Cr forms non-crystalline Cr_2O_3 on stainless steel by a direct reaction of Cr with H_2O and improves the resistance to localized corrosion.[2] Alloying with Mo enhances the protectiveness of a passive film to Cl^- by increasing oxygen affinity of the stainless steel.[3] Alloying with W inhibits localized corrosion by dissolved WO_4^{2-} from the passive film to an aqueous electrolyte or by forming insoluble WO_3, which enhances the stability of the passive film.[4] Alloying with N decreases local pH by decreasing acidity in pits due to NH_4^+ formation and promotes repassivation.[5] For ferritic stainless steel, however, the effect of N is not quite satisfied and usage of the simple PRE number (= wt% Cr + 3.3 wt% Mo) is proposed.[6] Although the PRE number is used for comparing localized corrosion resistances of various stainless steels, it is just an index and is not sufficient to provide kinetic information during localized corrosion. Kinetic information of localized corrosion must be related to the environmental conditions of initiation and/or propagation of localized corrosion as well as the composition of the material. Although there have been many studies on localized corrosion behavior of stainless steels in a solution containing Cl^-,[7–9] a precursor of the initiation of localized corrosion on stainless steel has not been fully elucidated. In order to understand the initiation of localized corrosion, it is necessary to investigate how Cl^- in solution acts as the precursor to degrade the passive film and to initiate localized corrosion.

Scanning electrochemical microscopy (SECM),[10] which can be used to estimate electrochemical reactivity at local sites of the electrode surface, has been applied to investigate the precursor of localized corrosion. The liquid-phase ion gun (LPIG) technique, which is a mode of SECM, is used to release controlled quantities of anions from a silver/silver-chloride microelectrode by cathodic polarization.[11] Fushimi et al. investigated the local breakdown mechanism of a passive film on iron by using the LPIG technique.[11] They reported that the breakdown of a passive film on iron depended on the substrate potential, electrical field applied to the film and pH of the solution.[12] Falkenberg et al. studied single pit initiation and its growth mechanism on a copper surface by using the combination of an electrochemical quartz crystal microbalance and an LPIG.[13] Gabrielli et al. investigated the pH dependence of the breakdown of a passive film on a pure iron surface by using an LPIG.[14] Since the quantity of Cl^- in the vicinity of the surface can be controlled electrochemically, the use of the LPIG technique is an alternative and/or advanced application to provide details about the initiation of localized corrosion of various materials.

In this study, the LPIG technique was applied to commercial ferritic stainless steels in Na_2SO_4 solution. The precursor processes of localized corrosion initiation were investigated, and the degrees of localized corrosion resistance of the stainless steels were also compared.

Experimental

Specimens.—Types 430 and 443J1 ferritic stainless steels were used as specimens. The chemical compositions of the stainless steels are shown in Table I. Stainless steel samples with a surface area of 1 cm^2 were mounted in epoxy resin, ground mechanically with SiC paper down to 1500 grit, rinsed with distilled water, and used as substrate electrodes for LPIG-mode SECM.

Table I. Chemical compositions of stainless steels used (wt%).

Type	Cr	Ti	Cu	C	N	Fe
430	16	-	-	0.05	0.03	bal.
443J1	21	0.3	0.4	0.01	0.01	bal.

*Electrochemical Society Member.
[z]E-mail: kfushimi@eng.hokudai.ac.jp

Potentiodynamic polarization.—Potentiodynamic polarization of the stainless steel electrode was performed from a less noble potential than the corrosion potential by −0.05 V to a noble potential at a scan rate of 1 mV s^{-1} in deaerated 0.15 mol dm^{-3} of Na_2SO_4 solution.

LPIG microelectrode.—An LPIG microelectrode for SECM was prepared by a procedure similar to that reported previously.[11,15] A silver wire (AG-401385, Nilaco) with a purity of 99.99% and a diameter of 500 μm was embedded in a glass capillary with an outer diameter of 1 mm using epoxy resin. A cross section of the silver-glass capillary tip was used as a silver microelectrode. After mechanical polishing with SiC papers down to 4000 grit and rinsing with distilled water, the microelectrode was polarized at 0.3 V against an Ag/AgCl/sat. KCl (SSE) reference electrode in 0.1 mol dm^{-3} NaCl solution at room temperature until a cathodic electric charge of 10 mC was consumed.

LPIG set-up.—An LPIG experiment for evaluating localized corrosion of stainless steel was carried out with an SECM set-up similar to that used previously.[11] The electrolyte solution used was 0.15 mol dm^{-3} of Na_2SO_4 solution deaerated by bubbling argon gas before measurements at room temperature. An LPIG microelectrode was positioned above the specimen electrode at a distance of 75 μm. The volume of the electrochemical cell was 100 cm^3. A platinum counter electrode with a surface area of 4 cm^2 and an SSE reference electrode were used. A bipotentiostat (HAL-1512 mM2, Hokuto Denko) was used to polarize both the specimen electrode and the LPIG microelectrode and to pass currents through them independently in the following manner. The potential of the LPIG microelectrode, E_{LPIG}, was initially kept at 0.3 V_{SSE} for 100 s and was then changed to −0.2 V_{SSE}, whereas the potential of the stainless steel electrode, E_{SS}, was controlled at 0.4 V_{SSE} throughout the experiment. The currents flowing through both electrodes were recorded at a rate of 10 Hz. In all electrochemical tests with an LPIG, the reproducibility was checked more than 3 times with different specimens.

Surface analyses.—The surfaces of the stainless steel specimens polarized at 0.4 V_{SSE} for 100 s with or without the LPIG operation were analyzed by Auger electron spectroscopy (AES; JAMP-9500F, JEOL) with a primary electron beam voltage at 10 keV. The specimen was rinsed with Mili-Q water after removing Na_2SO_4 solution. Ar^+ sputtering at an etching rate of 0.8 nm min^{-1} equivalent to silica was used for obtaining a depth profile of the local specimen surface with an electron beam diameter of 30 μm.

Numerical modeling.—The concentration distribution of Cl^- generated from the LPIG microelectrode against the specimen substrate electrode was simply considered as a diffusion problem with the assumptions that convection and migration are not effective for transporting chemical species and that no surface reaction occurs on the specimen surface. Fick's diffusion law is described as follows:

$$J = -D\nabla c, \qquad [1]$$

$$\partial c/\partial t = \nabla J = 0, \qquad [2]$$

where J is mass flux, t is time, and c and D are the concentration and diffusion coefficient of diffusing species, respectively. The time-dependent diffusion behavior of Cl^- generated from the LPIG with a two-dimensional geometry in a cylindrical coordinate system was modeled with finite element modeling (FEM). A commercial FEM solver, COMSOL Multiphysics 5.0, with a transport of diluted species module was used to solve the problem. The diffusion coefficients of H^+ and Cl^- used for modeling are 9.31×10^{-9} and 2.03×10^{-9} m^2 s^{-1}, respectively.[16] Current transient obtained in the LPIG experiment with the stainless steel was used to define the quantity of Cl^- generated from the LPIG microelectrode in FEM calculation.

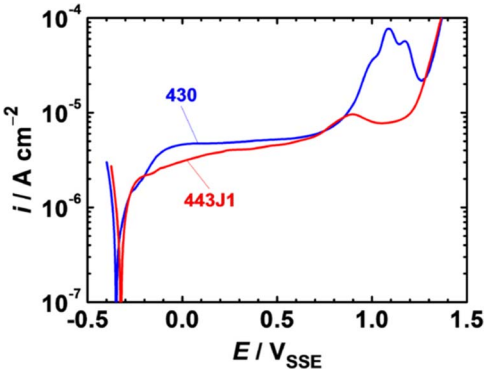

Figure 1. Potentiodynamic polarization curves of types 430 and 443J1 stainless steels in 0.15 mol dm^{-3} of Na_2SO_4 solution. Potential sweep rate was 1 mV s^{-1}.

Results

Electrochemical reaction of a silver microelectrode.—Electrochemistry of a silver microelectrode with or without a silver chloride layer was reported previously.[11] Anodic polarization of a silver electrode in a chloride-containing solution and cathodic polarization of a silver-silver chloride electrode correspond to the following reactions:[17]

$$AgCl + e^- \rightleftharpoons Ag + Cl^-. \qquad [3]$$

The latter reaction, reduction of AgCl, corresponds to generation of Cl^- from the LPIG. Although the diameter of the silver microelectrode used in this study was 500 μm, which is 2.8-times larger than that used previously,[11] anodic polarization of the LPIG microelectrode charged by the cathodic polarization with a charge of 10 mC could generate and discharge Cl^- with an anodic electric charge of 10 mC.

Anodic polarization of stainless steels.—Figure 1 shows polarization curves of types 430 and 443J1 stainless steels in 0.15 mol dm^{-3} Na_2SO_4 solution. Corrosion potential of type 443J1 stainless steel is slightly higher than that of type 430 stainless steel due to the higher amount of Cr, which makes the corrosion potential of stainless steel positive.[18] No active-passive transition is observed for the stainless steels, and the anodic current reaches a passive current lower than 4 μA cm^{-2} at potentials lower than ca. 0.7 V_{SSE}, implying that the specimen surface is spontaneously passivated before the polarization, probably just after specimen preparation. The passive current of type 430 stainless steel is larger than that of type 443J1 stainless steel, indicating that the passive film formed on type 430 stainless steel is less protective than that formed on type 443J1 stainless steel. At potentials higher than 0.69 V_{SSE}, the anodic current increases and shows a peak at 0.90 V_{SSE} for type 443J1 stainless steel and a peak at 1.09 V_{SSE} for type 430 stainless steel. This is attributed to the trans-passive oxidation of Fe, Cr or Ni in the oxide film and/or stainless steel substrate.[19,20] At higher potentials, the anodic current shows a trough and increases due to oxygen evolution. In this solution, no localized corrosion occurs on either of the stainless steels.

Current transients of LPIG and stainless steel during LPIG operation.—Figure 2 shows transients of the LPIG current I_{LPIG} and stainless steel substrate current I_{SS} observed in Na_2SO_4 solution when the LPIG potential E_{LPIG} was changed from 0.3 to −0.2 V_{SSE} at 100 s while the stainless steel specimen potential E_{SS} was kept at 0.4 V_{SSE}. Before the change of E_{LPIG}, no anodic current and only a small anodic current flow in the LPIG electrode and specimen electrode, respectively, indicating that the LPIG is in a standby to generate Cl^- and that the specimen surface is in a passive state. The I_{SS} at 100 s for type 430 stainless steel is larger than that for type 443J1 stainless steel. After the change of E_{LPIG} at 100 s, I_{SS} becomes larger because of the generation of Cl^-. A larger anodic current also starts to flow on stainless

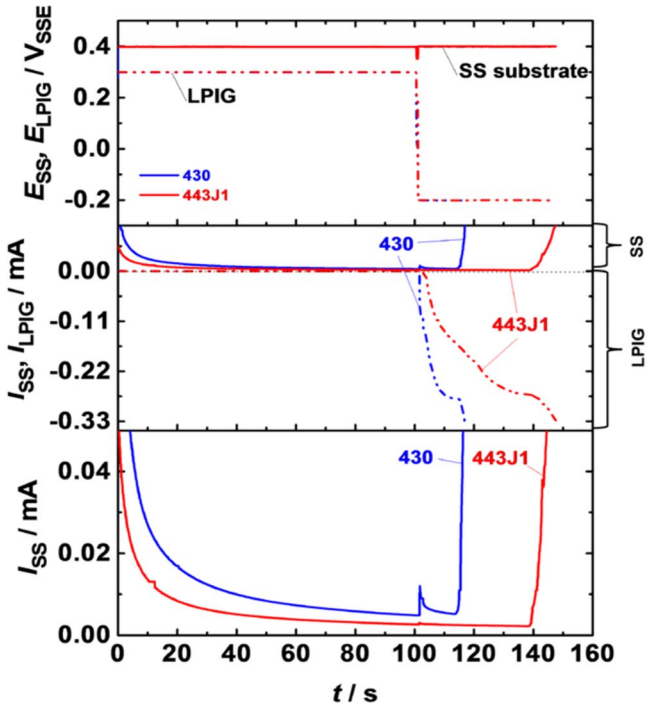

Figure 2. Transients of currents I_{LPIG} and I_{SS} of the LPIG microelectrode and stainless steel substrate electrodes, respectively, in 0.15 mol dm^{-3} of Na_2SO_4 solution when the electrode potential of the LPIG, E_{LPIG}, was changed from 0.3 to –0.2 V_{SSE} while the potential of the stainless steel substrate, E_{SS}, was kept at 0.4 V_{SSE}.

steel specimens. Furthermore, a slightly larger anodic current starts to flow on type 430 stainless steel at 0.72 s after the change of E_{LPIG} (t = 100.72 s). Increases in anodic current depending on the type of stainless steel should be correlated with some anodic processes on stainless steel and the operation of LPIG. Although non-faradaic processes including change in electric conductivity and/or capacitance in the interelectrode space due to the Cl^--concentrated environment and/or reorganization of the surface and double layer might be related to the increase in anodic current of the steel, it would be negligible because of the small time constant of the process. Meanwhile, strong dependency of the slightly increased current on the type of steel suggests that some faradaic processes should occur on the stainless steel surface. Degradation of the film is one of the processes and probably competes with the passivity-maintaining process of the surface. In the case of application of an LPIG to passivated pure iron in neutral solution,[11,12] dissolution of Fe(III) species from the passive film was observed during the initiation of film breakdown by concentrated Cl^- from the LPIG. Fe(III) species diffused to the LPIG were reduced and the so-called feedback phenomenon, repetition of the redox reaction of Fe(III) and Fe(II) between the microelectrode and degrading surface, occurred. If film degradation is initiated on the stainless steel surface due to the concentration of Cl^-, some alloying elements in the stainless steel might dissolve. However, the difference in I_{SS} on type 430 stainless steel in Na_2SO_4 solution is ca. 0.01 mA, which is significantly smaller than that in I_{LPIG}, ca. 0.2 mA. Therefore, little feedback of the redox reaction between Fe(III) and Fe(II) species is occurred on stainless steel in this study. Following the slight increase in current of type 430 stainless steel by the LPIG operation, on the other hand, I_{SS} rapidly increases at 12 s after the change of E_{LIPG} change (t = 112 s). Type 443J1 stainless steel suddenly allows an increase in anodic current flow at 39 s after the change of E_{LPIG} (t = 139 s). These large values of I_{SS} of the specimen electrodes imply the initiation and/or propagation of localized corrosion on stainless steel. In any case, it is considered that the time t_d from the change of E_{LPIG} to the rapid increase in I_{SS} corresponds to an induction period for the initiation of localized corrosion due to the LPIG operation. Additionally, the cathodic electric charge Q_d consumed by the LPIG electrode for t_d is considered to be the amount of Cl^- needed for the initiation of the corrosion. The relations between those parameters concerning the initiation of localized corrosion of stainless steel are discussed later.

Table II. Induction period t_d, cathodic electric charge Q_d, and concentration of chloride ions $[Cl^-]_d$ for initiation of localized corrosion obtained from the LPIG test and numerical modeling in 0.15 mol dm^{-3} Na_2SO_4 solution.

Type	t_d / s	Q_d / mC	$[Cl^-]_d$ / mol dm^{-3}
430	13 ± 1.1	2.5 ± 0.49	1.3
443J1	40 ± 8.3	7.0 ± 0.50	2.4

Parameters of localized corrosion initiation of stainless steels.—Table II shows parameters of localized corrosion initiation obtained by the LPIG test, including the induction time t_d cathodic electric charge Q_d needed for initiating localized corrosion and the critical concentration $[Cl^-]_d$. The LPIG prepared with a cathodic electric charge of 10 mC totally allows generation of 1.0×10^{-7} mol Cl^-. When the LPIG is located above the specimen surface with an interelectrode distance of 75 μm, a volume of ca. 1.0×10^{-7} dm^3 is estimated as an interelectrode solution between the LPIG and the specimen. Assuming that there is no Cl^- diffusion to the bulk solution during the LPIG operation, Cl^- with a mean concentration of 1.0 mol dm^{-3} can accumulate in the local solution. Numerical modeling is more effective to estimate Cl^--concentration $[Cl^-]$ at the specimen surface during the LPIG operation. Figure 3 shows the change in $[Cl^-]$ calculated numerically using transients of I_{LPIG} with an interelectrode distance of 75 μm in Na_2SO_4 solution. $[Cl^-]$ increases within 1 s after the commencement of cathodic polarization of the LPIG at 100 s. It is clear that the rate of increase is dependent on the specimen type. Type 430 stainless steel shows a larger rate than that of type 443J1 stainless steel. The maximum $[Cl^-]$ of 3.6 mol dm^{-3} delivered on the type 443J1 stainless steel surface is estimated at 160 s, though localized corrosion occurs on the stainless steel before the complete consumption of Cl^- on the LPIG microelectrode. In any case, the critical Cl^--concentration $[Cl^-]_d$ inducing local breakdown of the passive surface was determined. $[Cl^-]_d$ is clearly dependent on the steel type and type 443J1 is thought to be more resistive than type 430 because $[Cl^-]_d$ is about two-times higher in type 443J1. These parameters obtained for localized corrosion initiation correspond with the PRE number. Cr-rich type 443J1 shows larger t_d, Q_d, and $[Cl^-]_d$ than type 430.

Surface analyses of stainless steels.—Figure 4 shows AES depth profiles of specimen surfaces of types 430 and 443J1 stainless steels

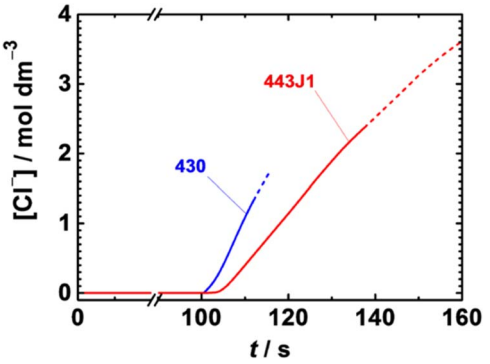

Figure 3. Change in Cl^--concentration $[Cl^-]$ at the specimen surface calculated numerically from the LPIG current in 0.15 mol dm^{-3} of Na_2SO_4 solution. $[Cl^-]$ after commencement of a rapid increase in I_{SS} is plotted by a dashed line.

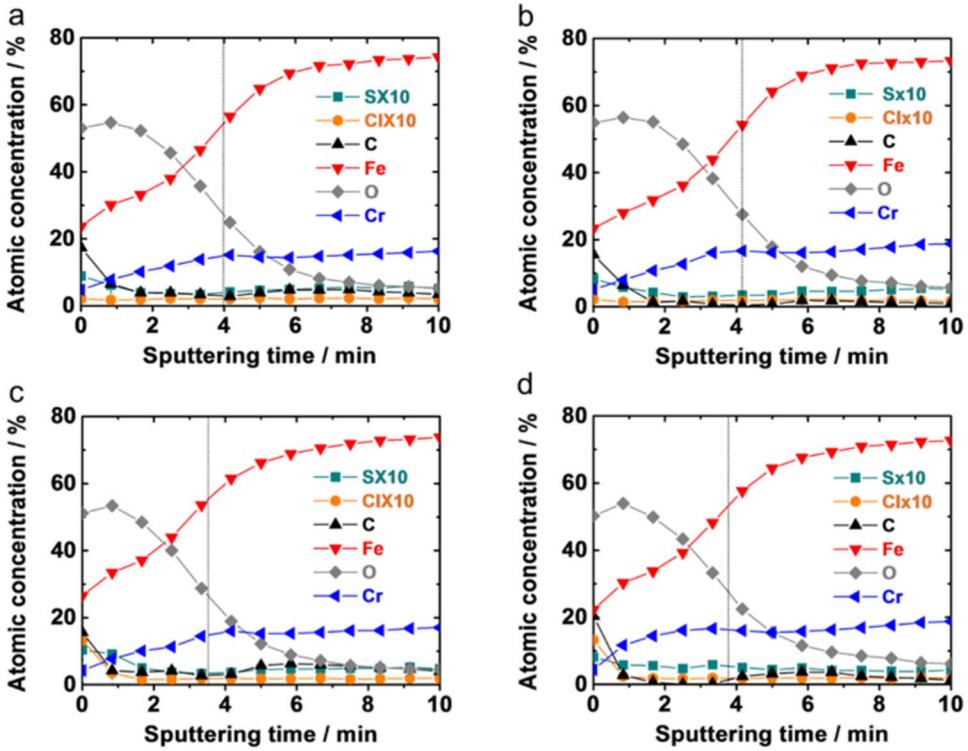

Figure 4. AES depth profiles of type 430 and 443J1 stainless steels polarized at 0.4 V_{SSE} in 0.15 mol dm^{-3} of Na_2SO_4 solution after operation of the LPIG consuming a cathodic electric charge. (a) 430, 0 mC, (b) 443J1, 0 mC, (c) 430, 1 mC, (d) 443J1, 1 mC.

polarized at 0.4 V_{SSE} in Na_2SO_4 solution after the operation of LPIG consuming a cathodic electric charge of 0 or 1 mC. Cl^--concentrations of 0.73 and 0.62 mol dm^{-3} are estimated from Figure 3 for 1 mC consumption of LPIG on types 430 and 443J1 stainless steels, respectively. It is clear from the presence of O with a high atomic concentration that the stainless steel surfaces were covered with oxide films. Assuming that the interface between the oxide film and substrate is located at the transition with a half of the atomic concentration of O, oxide films of both stainless steels formed at 0.4 V_{SSE} in Na_2SO_4 solution have thicknesses of ca. 3 nm. This is in good agreement with the previously reported thicknesses of 2 to 4 nm for passive films on stainless steels in aqueous solutions.[20–26] A small amount of S is contained in the outermost film of the stainless steels formed on both specimens, while Cl is only observed in the outermost film after the LPIG operation regardless of steel type. The S and Cl apparently originate from the solution and the LPIG, respectively. It is also clear from a comparison of Figures 4a and 4b and Figures 4c and 4d that thicknesses of passive films were ca. 10% smaller when the LPIG was operated and consumed a cathodic electric charge of 1 mC, indicating that the oxide film on stainless steels is thinned by contact with a Cl^--concentrated environment.

For both stainless steels, the atomic concentrations of Fe and Cr (Figures 5a and 5c) are larger in the oxide film formed with the LPIG operation than in the film formed without the LPIG operation, while the atomic concentration of O (Figures 5b and 5d) in the film with the LPIG operation is smaller than that in the film without the LPIG operation. The atomic concentration of Cl in the unsputtered films on both stainless steels is significantly higher than the detection limit (Figure 6). However, the atomic concentration of Cl is independent of the electric charge consumed by the LPIG microelectrode, indicating that Cl originating from the solution is only present in the outermost layer of the oxide film on the steel.

Similar AES depth profiling was also conducted for the surface of type 443J1 stainless steel that underwent the LPIG test with a cathodic electric charge of 2 mC. Figure 7 shows the film thicknesses of types 430 and 443J1 stainless steels as a function of the consumed cathodic electric charge in the LPIG operation. It is clear that the thickness of the film formed on both stainless steels gradually decreases with increase in the electric charge. Since localized corrosion progressed when the LPIG consumed a charge of 2 mC, the thickness cannot be plotted. However, the slope of type 443J1 stainless steel is gentler than that of type 430 stainless steel, indicating that degradation of the passive film formed on type 430 stainless steel occurs more easily than that of the passive film formed on type 443J1 stainless steel.

Discussion

The presence of Cl^- in the solution makes the passive film on stainless steel unstable and eventually results in localized corrosion.[27,28] The degradation of a passive film has been discussed using three major models concerning the role of Cl^-. (i) The adsorption model[29,30] is associated with the adsorption of Cl^- on the passive film surface. The adsorbed Cl^- accelerates the transfer of metal cations to the solution by forming a metal cation complex on the film, eventually thinning and removing the film. (ii) In the penetration model,[31,32] the depassivation of steel is due to the penetration of Cl^- through the film to the steel surface. The absorbed Cl^- introduces higher ionic conductive paths in the film, leading to a rapid transfer of metal cations to the solution. (iii) The breakdown model[33,34] is related to the mechanical stress accumulating in the film. The adsorption of Cl^- on the passive film reduces surface tension, resulting in mechanical breakdown of the passive film. As a result, degradation of the passive film exposed to the solution containing Cl^- is based on the adsorption of Cl^- on passive film surface. By the way, the PRE number has been used to rate the localized corrosion resistance of stainless steels, while the comparison of PRE number does not provide roles of Cl^- in a degradation of passive film before the initiation of localized corrosion on stainless steel. A more quantitative parameter concerning environmental effects of Cl^- should be used for the discussion. As states above, LPIG tests for types 430 and 443J1 stainless steels were carried out in Na_2SO_4 solution. The tests provided information about the induction process until the initiation of localized corrosion on both types of stainless steel.

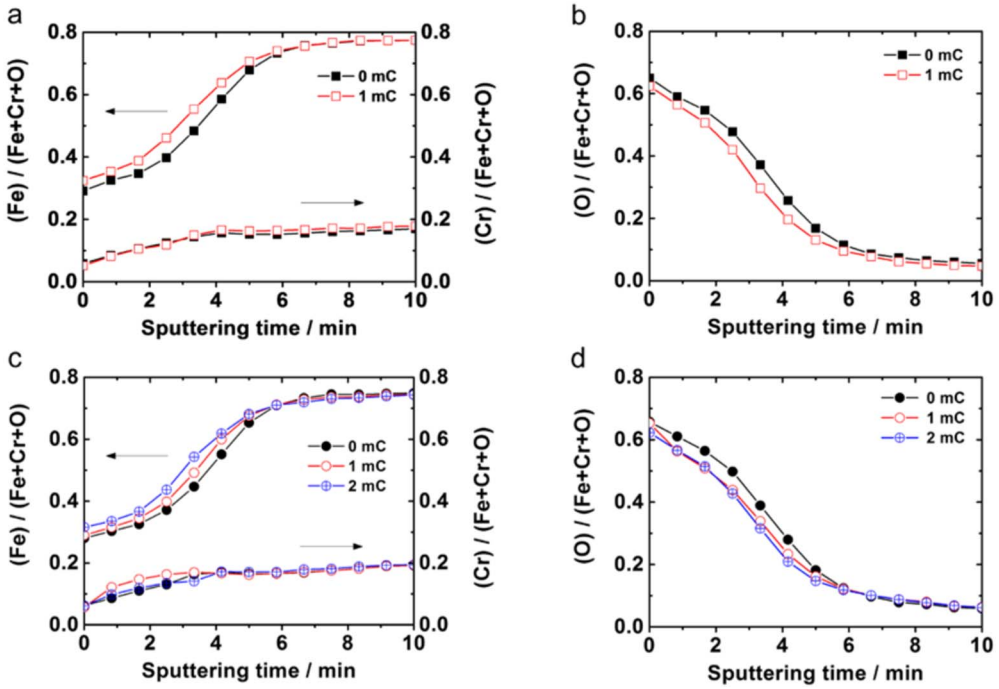

Figure 5. Atomic concentration ratios of Fe, Cr and O to the sum of these elements profiles of (a,b) type 430 and (c,d) type 443J1 stainless steels.

It is thought that the values of t_d and Q_d directly reflect the induction process of passive film breakdown and/or localized corrosion. The value of t_d is equivalent to incubation time for localized corrosion and the value of Q_d corresponds to the quantity of Cl^- needed for initiating localized corrosion. The critical Cl^--concentration $[Cl^-]_d$ needed for initiation of localized corrosion was obtained by numerical calculation using LPIG microelectrode current during the induction process. These electrochemical parameters are consistent with expectations obtained from the PRE number of stainless steel. Furthermore, AES analyses of the stainless steel surface following the LPIG operation revealed the existence of Cl on the outermost surface and a decrease in film thickness. This indicates that the adsorption of Cl^- on the oxide film and degradation of the film are caused by contact of the oxide surface with the Cl^--concentrated solution by the LPIG operation. The adsorbed Cl^- might support the transfer of metal cations, mainly Fe^{2+} and/or Fe^{3+}, in the film to the solution by forming a salt and/or complex on the film. Since solubilities of the salts $FeCl_2$ and $FeCl_3$ are 3.94 and 4.77 g, respectively, in 1 dm^3 water at 298 K,[35] the salt and/or complex spontaneously dissolves in an aqueous solution, suggesting that the presence of Cl^- at a high concentration in the solution results in dissolution of the film.

On the other hand, it has been reported that passive films formed on various ferritic stainless steels in aqueous solutions generally have an n-type semiconductive property.[25,36–38] Figure 8 shows schematic electron energy diagrams of the degradation process of a passive film during the operation of LPIG. In a solution without Cl^- (Fig. 8a), an oxide film that is composed of metal cations from the substrate and oxygen anions from the aqueous solution forms on the substrate, and it is subjected to an electric field and limits the anodic current flow. That is, the substrate is in a passive state. When the oxide film is in contact with the Cl^--concentrated solution by the operation of LPIG (Fig. 8b), however, Cl^- adsorbs on the film because Cl^- has about two times higher ability to adsorb on metal cation at film/solution interface than SO_4^{2-} or O^{2-}.[39] Salt and/or complex of chlorides forms in the outermost film and support the removal of metal cations in the film, resulting in an increase in the field applied to the film under a

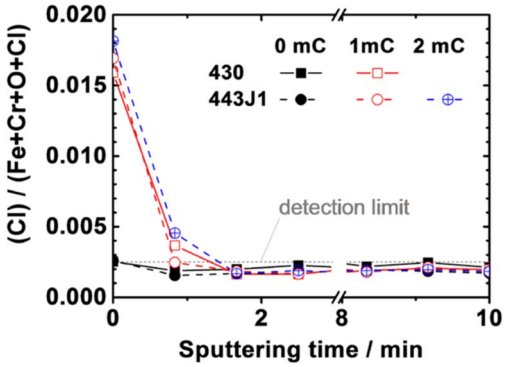

Figure 6. Atomic concentration ratio of Cl to the sum of major elements profiles of type 430 and 443J1 stainless steels. Detection limit was obtained from an average of atomic concentration of Cl in the oxide film in Figures 4a and 4b.

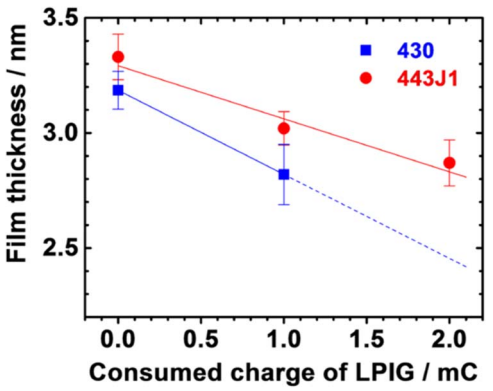

Figure 7. Thicknesses of oxide films formed on types 430 and 443J1 stainless steels as a function of cathodic electric charge consumed by the LPIG microelectrode.

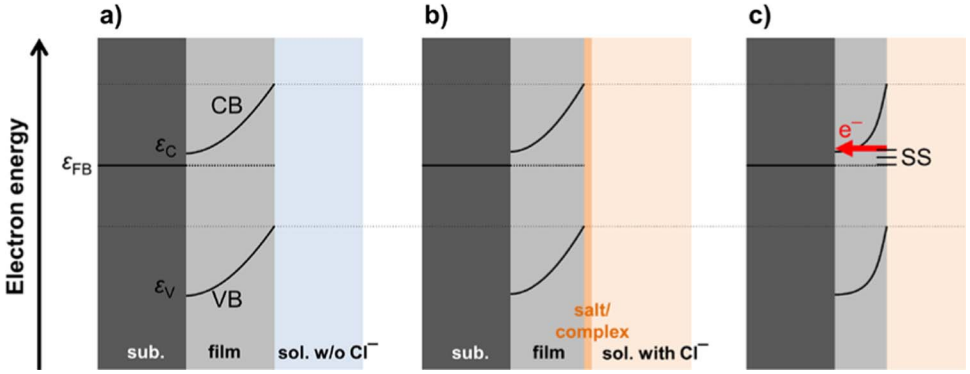

Figure 8. Schematic illustration of electron energy diagrams for localized corrosion initiation during the LPIG operation. (a) In a solution containing no Cl^-, the film formed on the substrate stands the electric field applied. (b) In a solution containing Cl^- at a high concentration, Cl^- adsorption on the film allows the formation of salt/complex layer at the film-solution interface. (c) Progress of complex formation and transfer of metal cations in the film lead to a band bending steeped by accelerated electron transfer from the surface state, SS, formed at the film-solution interface to the conduction band.

potentiostatic condition. This process affects further migration of cations and anions in the film. The dissolution of salt/complex competes with the repair of oxide film. In the case in which the dissolution rate is smaller than the repair rate, the film sustains the electric field and limits the current flow as a passive state. However, the film repaired is not completely as same as that before the dissolution. In that case, larger passive current might flow. When the dissolution rate is larger than the repair rate (Fig. 8c), in contrast, the thickness of the oxide film decreases and/or lead to form donor states, which are cation interstitials and/or anion vacancies, in the film. The damaged part experiences a higher electric field than the undamaged part. The migration of both anions and cations in the film is accelerated locally. The bands in the thin film become steep through these processes. Competitive reactions also lead to form surface states at the film/solution interface. They can provide additional paths of electric charge transfer in the space charge layer. When the oxide film allows an extraordinary electron transfer from surface states to the substrate through the conduction band of the oxide film, the dissolution of salt/complex is accelerated more and more since the electric charge transfer is more rapid than the ionic charge transfer for the oxide repair reaction. This process of film degradation corresponds to film breakdown or depassivation and proceeds until the film disappears.

Chromium oxides are superior to iron oxides for corrosion resistance in a Cl^--containing solution. The enrichment of chromium oxides in the oxide film formed on stainless steel improves the localized corrosion resistance.[40–44] A series of film degradation processes due to Cl^- adsorption on the film, i.e., formation of a chloride salt/complex and acceleration of substrate oxidation should be dependent on the concentration of Cr in the oxide film as well as the concentration of Cl^- at the film-solution interface. It is implied that the formation of chloride salt/complex is suppressed on chromium-rich oxides or the repair of oxide film is accelerated by portion of Cr content in stainless steel. It was confirmed in this study that the larger portion of Cr and/or the smaller portion of Fe in the oxide film formed on type 443J1 stainless steel than those in the film on type 430 stainless steel provide superior localized corrosion resistance.

Conclusions

Localized corrosion resistance of types 430 and 443J1 ferritic stainless steels polarized at 0.4 V_{SSE} in 0.15 mol dm^{-3} of Na_2SO_4 solution was evaluated by using the LPIG technique. As the LPIG microelectrode was cathodically polarized to generate Cl^-, the localized corrosion was initiated on both stainless steels. AES of stainless steel surfaces following the LPIG test revealed enrichment of Cl in the outermost layer of the oxide film and decreased film thickness due to contact with the Cl^--concentrated solution by the LPIG. Adsorption of Cl^- on the oxide film is thought to be a trigger of the dissolution and degradation of the passive film. The parameters obtained by the LPIG test, i.e., induction period t_d, cathodic electric charge Q_d and critical Cl^- concentration $[Cl^-]_d$ needed for the initiation of localized corrosion, are closely related to the PRE number of the stainless steel. The LPIG technique, which provides quantitative parameters concerning the role of Cl^- during the induction period, is useful for investigating the initiation of localized corrosion of stainless steels.

Acknowledgments

This work was conducted at Hokkaido University and supported by JFE Steel Corp., "Nanotechnology Platform" Program of the Ministry of Education, Culture, Sports, Science and Technology (MEXT), Japan, a Grant-in-Aid for Scientific Research (B) 25289235 of Japan Society for Promotion of Science (JSPS) and JSPS fellowship by a Grant-in-Aid for No. 260061.

References

1. H. Okamoto, *Proc. Conf. Application of Stainless Steels '92*, 360, The Institute of Materials, Stockholm, Sweden (1992).
2. A. B. Brooks, C. R. Clayton, K. Doss, and Y. C. Lu, *J. Electrochem. Soc.*, **133**, 2459 (1986).
3. K. Sugimoto and Y. Sawada, *Corros. Sci.*, **17**, 425 (1977).
4. H. Baba, T. Kodama, and Y. Katada, *Corros. Sci.*, **44**, 2393 (2002).
5. N. Bui, A. Irhzo, F. Dabosi, and Y. Limouzin-Maire, *Corrosion*, **39**, 491 (1983).
6. Y. Yazawa, T. Ujiro, S. Satoh, and K. Yoshioka, *Zairyo-to-Kankyo*, **44**, 654 (1995).
7. N. J. Laycock and R. C. Newman, *Corros. Sci.*, **40**, 887 (1998).
8. G. Salamat, G. A. Juhl, and R. G. Kelly, *Corrosion*, **51**, 826 (1995).
9. S. Marcelin, N. Pébère, and S. Régnier, *Electrochim. Acta*, **87**, 32 (2013).
10. A. J. Bard, F.-R. F. Fan, J. Kwak, and O. Lee, *Anal. Chem.*, **61**, 132 (1989).
11. K. Fushimi, K. Azumi, and M. Seo, *J. Electrochem. Soc.*, **147**, 552 (2000).
12. K. Fushimi and M. Seo, *J. Electrochem. Soc.*, **148**, B450 (2001).
13. F. Falkenberg, K. Fushimi, and M. Seo, *Corros. Sci.*, **45**, 2657 (2003).
14. C. Gabrielli, S. Joiret, M. Keddam, N. Portail, P. Rousseau, and V. Vivier, *Electrochim. Acta*, **53**,7539 (2008).
15. J.-S. Lee, K. Fushimi, Y. Kitagawa, T. Nakanishi, and Y. Hasegawa, *J. Electrochem. Soc.*, **162**, C115 (2015).
16. D. R. Linde, *CRC Handbook of Chemistry and Physics* 72th edition, 5–970, CRC Press, Boca Raton (1992).
17. A. J. Bard, R. Parsons, and J. Jordan, *Standard Potentials in Aqueous Solutions*, Marcel Dekker, New York (1985).
18. I. Olefjord And B.-O. Elfstrom, *Corrosion*, **38**, 46 (1982).
19. C.-J. Park, H.-S. Kwon, and M. M. Lohrengel, *Mater. Sci. Eng. A*, **372**, 180 (2004).
20. M. Kumagai, S-T. Myung, S. Kuwata, R. Asaishi, and H. Yashiro, *Electrochim. Acta*, **53**, 4205 (2008).
21. M. G. S. Ferreira and J. L. Dawson, *J. Electrochem. Soc.*, **132**, 760 (1985).
22. G. Lorang and M. D. C. Belo, *J. Electrochem. Soc.*, **141**, 3347 (1994).
23. D. Wallinder, J. Pan, C. Leygraf, and A. Delblanc-Bauer, *Corros. Sci.*, **41**, 275 (1999).
24. A. Atrens, *J. Electrochem. Soc.*, **144**, 3697 (1997).
25. M. J. Carmezim, A. M. Simões, M. F. Montemor, and M. De Cunha Belo, *Corros. Sci.*, **47**, 581 (2005).
26. I. Olefjord and L. Wegrelius, *Corros. Sci.*, **31**, 89 (1990).
27. A. R. Brooks, C. R. Clayton, K. Doss, and Y. C. Lin, *J. Electrochem. Soc.*, **133**, 2459 (1986).

28. N. Sato, *Corrosion*, **45**, 354 (1989).
29. J. A. Kolotyrkin, *Corrosion*, **19**, 261t (1963).
30. T. P. Hoar and W. R. Jacob, *Nature*, **216**, 1299 (1967).
31. R. R. Evans, *J. Chem. Soc.*, 1020 (1927).
32. T. P. Hoar, D. C. Mears, and G. P. R. Rothwell, *Corros. Sci.*, **5**, 279 (1965).
33. T. P. Hoar, *Corros. Sci.*, **7**, 341 (1967).
34. N. Sato, *Electrochim. Acta*, **16**, 1683 (1971).
35. W. M. Haynes, *CRC Handbook of Chemistry and Physics* 92th edition, 5–192, CRC Press, Boca Raton (2011).
36. C. Sunseri, S. Piazza, A. D. Paola, and F. D. Quarto, *J. Electrochem. Soc.*, **134**, 2410 (1987).
37. N. E. Hakiki and M. D. C. Belo, *J. Electrochem. Soc.*, **146**, 3088 (1996).
38. Y. Wang, S. L. Jiang, Y. G. Zheng, W. Ke, W. H. Sun, and J. Q. Wang, *Corros. Sci.*, **63**, 159 (2012).
39. J. M. West, *Electrodepositon and Corrosion Process*, 114, The Camelot Press Ltd., London and Southampton (1965).
40. A. J. Sedriks, *Corrosion*, **42**, 377 (1986).
41. J. E. Castle and J. H. Qiu, *J. Electrochem. Soc.*, **137**, 2031 (1990).
42. H. Ogawa, H. Omata, I. Itoh, and H. Okada, *Corrosion*, **34**, 52 (1978).
43. N. E. Hakiki, S. Boudin, B. Rondot, and M. D. C. Belo, *Corros. Sci.*, **37**, 1809 (1995).
44. C.-O. A. Olsson and D. Landolt, *Electrochim. Acta*, **48**, 1093 (2003).